

# Fundamental studies on a planar-cathode direct current glow discharge. Part I: characterization via laser scattering techniques<sup>☆</sup>

Gerardo Gamez<sup>a</sup>, Annemie Bogaerts<sup>b</sup>, Francisco Andrade<sup>a</sup>, Gary M. Hieftje<sup>a,\*</sup>

<sup>a</sup>Department of Chemistry, Indiana University, Bloomington, IN 47405, USA

<sup>b</sup>Department of Chemistry, University of Antwerp, Universiteitsplein 1, B-2610 Wilrijk-Antwerp Belgium

Received 30 September 2003; accepted 3 December 2003

## Abstract

A laser-scattering-based instrument was used to study an argon d.c. planar-diode glow discharge. The gas-kinetic temperature ( $T_g$ ) was determined via Rayleigh scattering and the electron number density ( $n_e$ ), electron temperature ( $T_e$ ), and shape of the electron energy-distribution function were determined by Thomson scattering. Axial profiles of these parameters were obtained as the discharge current, voltage, and pressure were varied. Trends in the profiles of  $T_g$  and in the other parameters show the interdependence of these plasma species and properties. The results will be compared with current theoretical computer models in order to improve our understanding of the fundamental processes in glow discharges sustained under conditions appropriate for spectrochemical analysis.

© 2003 Elsevier B.V. All rights reserved.

**Keywords:** Thomson scattering; Rayleigh scattering; Glow discharge; Gas-kinetic temperature; Electron number density; Electron temperature; Electron energy distribution function

## 1. Introduction

Glow discharges are commonly used in analytical spectrochemistry as sources of atoms and ions, especially from solid samples [1–3]. However, even though there have been many fundamental studies aimed at characterizing the glow discharge, we are still far from fully understanding the behavior of the different plasma species and how they are affected by discharge operating conditions. In order to acquire greater insight into the mechanisms of fundamental plasma processes we must continually strive for better agreement between the most current glow discharge computer models and experimental observations.

A great number of fundamental experiments on glow discharges have been performed in the past. Of particular interest are those that report the electron behavior and plasma gas temperature, because these properties are no doubt tied to the pressure, voltage and current characteristics of the plasma as well as to the excitation, ionization, and sputtering processes. For example, the electron properties have been observed by means of Langmuir probes or by following the Stark broadening of the  $H_\beta$  line or even the He 447.148 nm line [4–8]. It is worth noting that fundamental studies performed by different experimental methods sometimes differ in their observations. A possible contribution to these differences may be the sources of error from each technique. For example, Langmuir probes have been known to perturb the plasma [9]. Similarly, Abel inversion (a mathematical technique that introduces error) must be used in order to obtain radially resolved values from the measurements of Stark broadening of the  $H_\beta$ -line. Other factors that may contribute to the discrepancies may be differences in operating conditions or source configuration. It is therefore important to probe the electron properties by other means and under differ-

<sup>☆</sup>This paper was presented at the Presymposium on Sample Introduction in Atomic Spectrometry of the Colloquium Spectroscopicum Internationale XXXIII in Spain. The presymposium was held in Zaragoza, 3–6 September 2003. This paper is published in the special issue of *Spectrochimica Acta Part B*, dedicated to the CSI XXXIII.

\*Corresponding author. Tel.: +1-812-855-2189; fax: +1-812-855-0958.

E-mail address: [hieftje@indiana.edu](mailto:hieftje@indiana.edu) (G.M. Hieftje).

ent operating conditions in order to have an enhanced database to compare to current theoretical models. In addition, the gas-kinetic temperature in glow discharges has been studied previously by means of Doppler broadening,  $N_2^+$  and OH rotational emission, thermocouple, and via a manometer probe [10–12]. However, the reported temperatures differ. Thus, it is crucial to confirm such observations by other methods.

For this purpose, an instrument was recently designed by Gamez et al. [13] to map electron densities ( $n_e$ ), electron energy distribution functions (EEDF), electron temperatures ( $T_e$ ), and gas-kinetic temperatures ( $T_g$ ) in a d.c. planar-cathode glow discharge. Thomson scattering of laser radiation is used to observe the electron properties and Rayleigh scattering to measure the gas-kinetic temperature. Laser scattering does not suffer from the same flaws as the previously mentioned techniques, as long as the laser power is held below the threshold to cause plasma heating. In addition, with laser-scattering techniques  $T_e$  and  $n_e$  are obtained independently, there is inherent spatial resolution, and there exists the possibility of temporal resolution. Thus, it is an excellent alternative method to study analytical glow discharges.

The purpose of the present study is to use this laser-scattering instrument to characterize the glow discharge over a range of operating conditions of analytical interest. Specifically,  $n_e$ ,  $T_e$ , EEDF and  $T_g$  were studied as a function of axial distance from the cathode while the discharge operating parameters of pressure, current and voltage were varied. Particular emphasis was placed on the negative-glow region. The results are compared to observations performed earlier with different techniques. In addition, a parallel study (which we will refer to as paper II) was performed where a numerical model is applied to the same operating conditions and a comparison to the experimental results is made [14].

## 2. Experimental

The laser-scattering diagnostics instrument, designed for measurements on a glow discharge, has already been described in some detail [13], so only a brief overview is appropriate here. A double monochromator is used for high stray-light rejection. In addition, a gated photon-counting system is employed to further reduce the stray light detected and to be able to measure the weak Thomson-scattering signals.

The glow discharge is sustained between a planar copper cathode (1.2-cm diameter) and a stainless-steel anode (5.0-cm diameter), which are positioned 5.0 cm apart. The cathode is electrically insulated by a Macor<sup>®</sup> piece and the anode by Delrin<sup>®</sup>. The glow discharge cell is floated electrically. The cathode is held by a brass piece cooled by a chiller set to 13 °C. The plasma gas is argon and the flow is 0.14 l/min at 1 Torr and 0.36 l/min at 3 Torr.

The glow discharge was operated in the abnormal mode. As a consequence, the sustaining voltage rises in proportion to the operating current and the power applied to the discharge changes proportionally with the square of the current. Further, it would be expected that the sample erosion rate would be dependent on the current density at the sample surface, in terms of mA/cm<sup>2</sup>, and that some other parameters in the discharge would be related to the power density at the sample, in terms of W/cm<sup>2</sup>. To simplify comparison with theoretical models later, current density and power density figures will be cited below, along with the conventional values for operating current and voltage.

For all the features that were measured an axial profile was obtained. In these measurements, the laser is held in place while both the cathode and anode pieces are moved, thus altering the observation distance with respect to the cathode. The observation distances studied here include 23, 18, 13, 8, 6, and 4 mm from the cathode, thus ensuring that the negative glow region was probed. Measurements below 4 mm could not be performed due to high levels of stray light.

Gas-kinetic temperatures were determined at 2.5 (2.2 mA/cm<sup>2</sup> or 1.2 W/cm<sup>2</sup>) and 10 mA (8.9 mA/cm<sup>2</sup> or 7.8 W/cm<sup>2</sup>) while the pressure was kept at 1 Torr. At 3 Torr, measurements were taken at 10, 30, 50, and 65 mA (8.9, 26.6, 44.3, 58 mA/cm<sup>2</sup> or 3.8, 17.1, 34, 58 W/cm<sup>2</sup>, respectively). Measurements at 3 Torr and 2.5 mA were not obtained because the negative glow was smaller than 4 mm under these conditions. Thomson-scattering spectra were acquired at both 55 and 35 mA while the pressure was kept at 3 Torr. Also, a set of axial Thomson scattering spectra were acquired at 1 Torr and 5 mA. The discharge was always operated in a current-limited mode and the resulting voltages are reported on the Results and discussion section.

In addition, an experiment to gauge the cathode surface temperature was performed. Four 1-mm i.d. holes were drilled 4 mm from the center on the back of the cathode; the bottom of each hole was approximately 0.3 mm from the cathode surface. Metal shavings chosen according to their melting points were placed in these 'wells'. The metals used were Zn, Pb, Bi, Sn, and In (m.p. 692.68 K, 600.61 K, 544.55 K, 505.08 K, and 429.75 K, respectively) [15].

The cathode was pre-sputtered for 20 min at 1 Torr and 2.5 mA before every set of measurements. In addition, a 5 to 10 min discharge-stabilization period was allowed each time the operating conditions were changed. All measurements were performed in triplicate for statistical purposes.

## 3. Results and discussion

### 3.1. Gas-kinetic temperature

Heating of the plasma gas in a glow discharge can arise from several collisional processes. For example,

ions accelerated towards the cathode will collide with neutrals and the resulting fast neutrals will in turn collide with slow neutrals [16,17]. In this manner, the applied electrical energy is redistributed and ultimately raises the temperature of the thermalized neutrals. Another likely contribution to gas heating arises from collisions between sputtered neutrals and the plasma background gas. In addition, it has been suggested that collisions between electrons and the plasma–gas species might promote gas heating, assuming these are frequent enough, despite the considerable mass difference between the collision partners [16]. In contrast, Bogaerts et al. [18] found through theoretical computer modeling that collisions with electrons play a minor role for gas heating under analytical glow discharge conditions.

The gas-kinetic temperature in a glow discharge can play a very important role. For example,  $T_g$  is inversely related to the gas density, a parameter that influences the frequency of collisions, which in turn affects ionization kinetics and the electron density [18]. In this manner, the gas-kinetic temperature will have an effect upon the global electrical characteristics of the plasma. Thus, it is critical to measure the gas temperature in the plasma in order better to understand the plasma processes.

When taking temperature measurements in low-pressure plasmas, one must bear in mind that there might not be enough collisions to produce local thermodynamic equilibrium (LTE). In fact, the glow discharge is considered not to be in LTE. This translates operationally to different temperatures for different species or even to non-Maxwellian or non-Boltzmann behavior. Thus, excitation temperatures are not really useful other than for obtaining a measure of the energy distribution of particular species [10].

In order to obtain an approximation of the gas-kinetic temperature in a glow discharge, researchers have resorted to using either rotational temperatures from nitrogen moieties or OH, or Doppler broadening from absorption or emission of plasma species [10,11,7,8]. The drawback of approximating gas temperatures from rotational spectra of molecular species is that it is necessary to add enough of those species to obtain a measurable spectrum, which can in turn alter the temperature. For example, Ohorodnik and Harrison [10] showed that addition of  $N_2$  to a glow discharge reduced the measured temperature. In addition, Abel inversion is needed in order to obtain radically resolved values from both rotational temperatures and Doppler-broadening measurements, which, as stated before, will introduce some error. Other authors have resorted to using thermocouples or pressure probes [10,12]. Obviously, these methods will perturb the plasma.

Muraoka et al. [16,19] pioneered the use of Rayleigh scattering to determine the plasma gas density in low-pressure processing plasmas. Gamez et al. [13] introduced the use of this technique for glow discharges

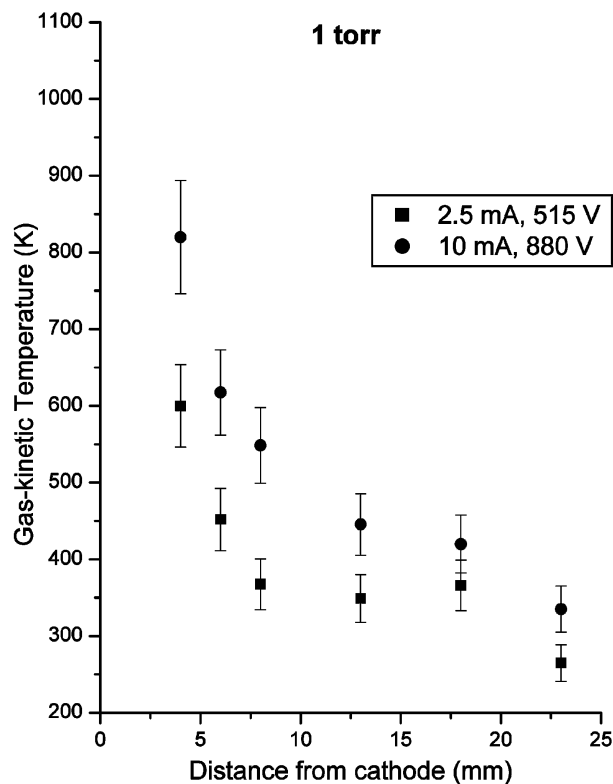


Fig. 1. Gas-kinetic temperature as a function of distance from the cathode on the plasma axis at 1 Torr of argon.

intended for analytical purposes. As mentioned earlier, Rayleigh scattering has several advantages but it may be limited in accuracy by the presence of species with larger Rayleigh-scattering cross-sections than the species of interest. In the present case, argon metastables are the species that might affect the integrity of the Rayleigh scattering. However, based on the argon metastable density reported in other studies performed under similar conditions [11,20–23], we believe this is not a concern in our measurements. Due to the technique's simplicity and its complementarity to Thomson scattering it has been our method of choice.

Fig. 1 shows the gas-kinetic temperature determined at 1 Torr while the current was kept at 2.5 (515 V, 2.2 mA/cm<sup>2</sup>, 1.2 W/cm<sup>2</sup>) and 10 mA (880 V, 8.9 mA/cm<sup>2</sup>, 7.8 W/cm<sup>2</sup>). It is evident that as the current and voltage go up the gas-kinetic temperature follows. However, there appear to be three distinct spatial regions of behavior. From 4 to 8 mm from the cathode the temperature gradient is very steep (820–550 K at 10 mA, 600–370 K at 2.5 mA). This is still within the negative glow region. Then, there is a zone between 8 and 18 mm from the cathode where the temperature is relatively constant at approximately 350 K at 2.5 mA and where the decrease is not as pronounced at 10 mA. Finally, at 23 mm from the cathode there is another abrupt drop to near room temperature. Measurements

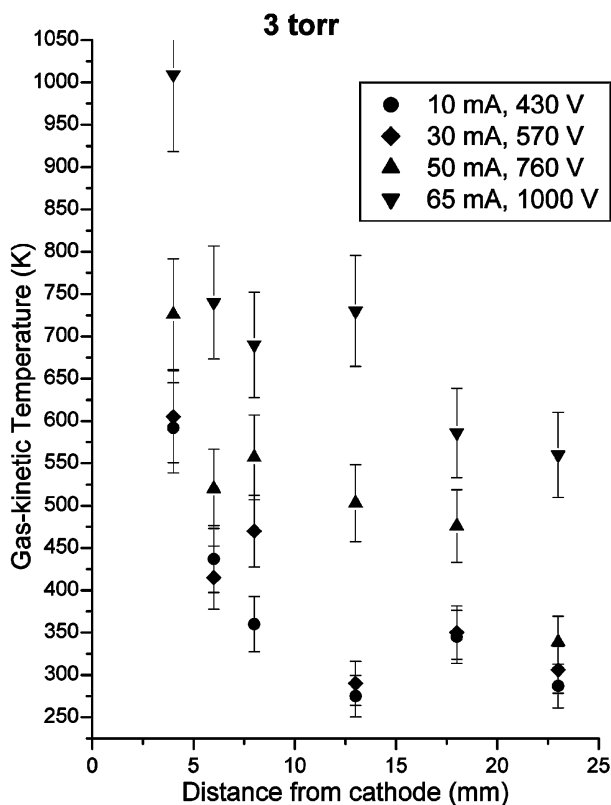


Fig. 2. Gas-kinetic temperature as a function of distance from the cathode on the plasma axis at 3 Torr of argon.

below 4 mm were not possible because of high levels of stray light from the cathode insulator.

The effect of pressure on the gas-kinetic temperature was also determined. When the pressure was raised from 1 to 3 Torr (cf. Fig. 2) there was a drop in temperature for the same operating current (cf. points for 10 mA). Of course, the sustaining voltage was lower for the same operating current at the higher pressure; as a result the power at 1 Torr and 10 mA was  $\sim 8.8$  W while the power at 3 Torr and 10 mA was only  $\sim 4.3$  W. Based on Ohm's law we can say that the increment in pressure, which produces a lower voltage, leads to a drop in resistance which translates to a reduced plasma–gas temperature.

Because of the inverse relationship between pressure and sustaining voltage, the voltage limit of the power supplier was reached at lower currents at 1 Torr than at 3 Torr. As a result, we were able to apply higher power levels at 3 Torr. Again, the gas-kinetic temperature went up as the current was raised. At 3 Torr–10 mA ( $8.9$  mA/cm<sup>2</sup>,  $3.8$  W/cm<sup>2</sup>) and 3 Torr–30 mA ( $26.6$  mA/cm<sup>2</sup>,  $17.1$  W/cm<sup>2</sup>) the temperatures are comparable to those observed at 1 Torr and 2.5 mA. The change in gas temperature with distance from the cathode also exhibited the same precipitous drop. However, at the highest operating powers (3 Torr–50 mA,  $44.3$  mA/cm<sup>2</sup>,  $34$  W/

cm<sup>2</sup>; and 3 Torr–65 mA,  $58$  mA/cm<sup>2</sup>,  $58$  W/cm<sup>2</sup>) there was a higher  $T_g$  at greater distances from the cathode than for either of the applied current levels at 1 Torr. In addition, these higher-power conditions give a broader zone (above 6 mm from the cathode) where the change in temperature is not as dramatic as at lower power. It is useful to note that at 1 Torr, a side-view visual inspection revealed that the negative glow extended roughly 10 mm from the cathode at 2.5 mA and approximately 20 mm at 10 mA. Beyond the negative glow a halo characterized by a purple color was evident. At 3 Torr and 10 mA, the negative glow was smallest (to approx. 6 mm from the cathode) and grew as the current was raised (at 30 mA, approx. 15 mm; at 50 mA, approx. 18 mm; and at 70 mA, approx. 23 mm). In the 3 Torr case, a halo characterized by a green color was evident.

This behavior seems intuitively reasonable and agrees fairly well with results from previous studies when differences in the glow discharge geometry and experimental conditions are taken into account. For example, West and Human [24] measured chromium Doppler temperatures in a Grimm-type glow discharge and saw an increase in temperature as the current was raised. Under the most closely comparable conditions, 25 and 50 mA, they measured temperatures approximately 1000 K and 1400 K, respectively, at 1000 V. Ferreira et al. [7] reported argon Doppler temperatures from a side-view Grimm-type glow discharge which, regardless of the operating conditions, declined abruptly within the first millimeter from the cathode (to approx. 400 K) and then changed very little until 4 mm (the greatest distance examined). The reported temperatures ranged from  $\sim 1800$  K (at  $148$  W/cm<sup>2</sup>) to  $\sim 900$  K (at  $93$  W/cm<sup>2</sup>). Kuraica et al. [8] also reported argon Doppler temperatures from a Grimm-type source, which varied from  $\sim 1200$  K (at  $57$  W/cm<sup>2</sup>) to  $\sim 500$  K (at  $20$  W/cm<sup>2</sup>) depending on the operating conditions. Furthermore, they showed that at lower power settings the temperature drops abruptly within the first 7 mm from the cathode but that at higher powers the decrease is no longer observable between 3 and 7 mm from the cathode. The rotational temperatures reported by Oho-rodnik and Harrison [10] for a d.c. glow discharge at 1 Torr and 4 mA go from  $\sim 575$  to  $\sim 525$  K within the first 3 mm from the cathode. For the same operating conditions, they used a thermocouple and measured temperatures from  $\sim 430$  to  $\sim 320$  K from 0 to 25 mm from the cathode. As in our case, they saw the greatest drop in temperature within the negative glow under similar conditions. Finally, Bogaerts et al. [18] used a Monte Carlo and heat-transfer model to calculate the temperature in a Grimm-type glow discharge and obtained temperatures from  $\sim 1050$  K (at approx.  $120$  W/cm<sup>2</sup>) to room temperature that were shown to depend on the pressure and cathode temperature. They also

show a sizable drop in temperature within the vicinity of the cathode, which then comes to a plateau close to room temperature. This is similar to what we see at 1 Torr. In addition, as the current was elevated they observed a larger contribution of the sputtered-atom collisions to gas heating. For the conditions under study here, the calculated values are in reasonable agreement with the experimental data, as will be shown in paper II [14].

As mentioned above, Bogaerts et al. [18] found a strong interdependence between the gas kinetic temperature and the cathode surface temperature in their numerical models. In addition, Kasik et al. [25] found differences in I–V characteristics that they attributed to cathode temperature. Consequently, we performed an experiment to estimate the cathode surface temperature. Pure metal shavings were placed in small wells (drilled on the back of the cathode) whose bottom was very close (approx. 0.3 mm) to the cathode surface. After 30 min of running the discharge under the conditions of interest we examined the metal shavings for signs of melting. By determining which metals melted and which did not we can establish a range for the cathode surface temperature. This method has the advantage of being cost-effective and simple. In addition, there is no need for independent calibration. However, we can obtain only an approximate range for the cathode surface temperature.

In order, to validate this method we removed the cathode assembly from the discharge chamber and positioned it so the cathode surface was flat against the top of a hot plate. A small gap was made on the cathode surface to enable a thermocouple to be inserted between the cathode and the hot plate. The hot plate was heated to the point that the thermocouple indicated 438 K at the same time the cathode assembly was cooled in the same fashion as when the discharge is being operated. Under these conditions, only the In shavings (m.p. 430 K) melted, indicating that the method closely estimates the cathode surface temperature.

When the discharge was operated at 3 Torr and 65 mA, In, Sn and Bi shavings melted but not Pb nor Zn. This indicates that the temperature at the cathode surface under these conditions is between 544.55 and 600.61 K. This information will become critical when these experimental results are compared to numerical models (see paper II [14]).

### 3.2. Electron properties

As was stated earlier, electron properties are involved in several important plasma processes. For example, electron-impact excitation and ionization of the plasma gas and of sputtered analyte atoms depend on the electron concentration and energy distribution. Also, certain other ionization processes, such as Penning

ionization and fast argon-ion and argon-atom impact ionization, will yield electrons having particular properties [3]. In addition, ion and metastable bombardment of the cathode surface will induce secondary electron emission [3]. Moreover, the electron flux strongly influences the global electronic properties of the discharge. For instance, the current is mainly carried by electrons in the negative-glow region [3].

Electron properties obtained from Thomson-scattering spectra include  $n_e$ , the shape of the EEDF, and  $T_e$ . Fig. 3 shows linearized [26] Thomson scattering spectra taken at various distances from the cathode under operating conditions of 3 Torr and 55 mA. When the spectra are plotted in this fashion they will yield a straight line if the electron energy distribution is Maxwellian; from the slope of this line we can derive  $T_e$  [26]. As Fig. 3 shows, there arises a greater and greater degree of non-Maxwellian behavior as the observation height approaches the cathode. The spectra at 4, 6, and 8 mm from the cathode display high-energy tails that have clearly different slopes than the data at smaller wavelength shifts (lower electron energies). Since the linear fit of the tails is fairly good and because other authors have reported the existence of several electron classes with distinct energy distributions, we will assume here a bi-Maxwellian distribution that should yield a good estimate of the energies of the different electron groups in the discharge [6,27]. Importantly, since thermalized (low-energy) electrons contribute much more to the Thomson scattering spectrum than do those in the high-energy tail, the effect of this assumption on the derived temperatures for the thermalized group will be insignificant.

Electron temperatures derived from the slopes of the first squared wavelength-shift channels of the spectra are approximately 0.3 eV. These correspond to the energies of thermalized electrons [3,27]. In fact, at greater distances from the cathode (13 and 18 mm), where only a single electron group appears to exist, the whole linearized spectrum can be fitted with a single line for which the determined temperature is near 0.3 eV. Closer to the cathode, the temperature derived from the high-energy tails of the linearized spectra go from 1.36 eV at 4 mm to 1.49 eV at 6 mm and finally to 0.83 eV at 8 mm. Electrons arising from gas-phase ionization events usually have energies ranging from ~2–10 eV [27]. Thus, the temperatures of the high-energy group of electrons correspond to gas-phase ionization electrons that have been involved in a few collisions. Furthermore, the temperature decrease of the high-energy electron group from 6 to 8 mm shows how they undergo ever more collisions while traveling through the negative glow. Finally, at even greater distances from the cathode the electrons appear to have undergone enough collisions to become fully thermalized.

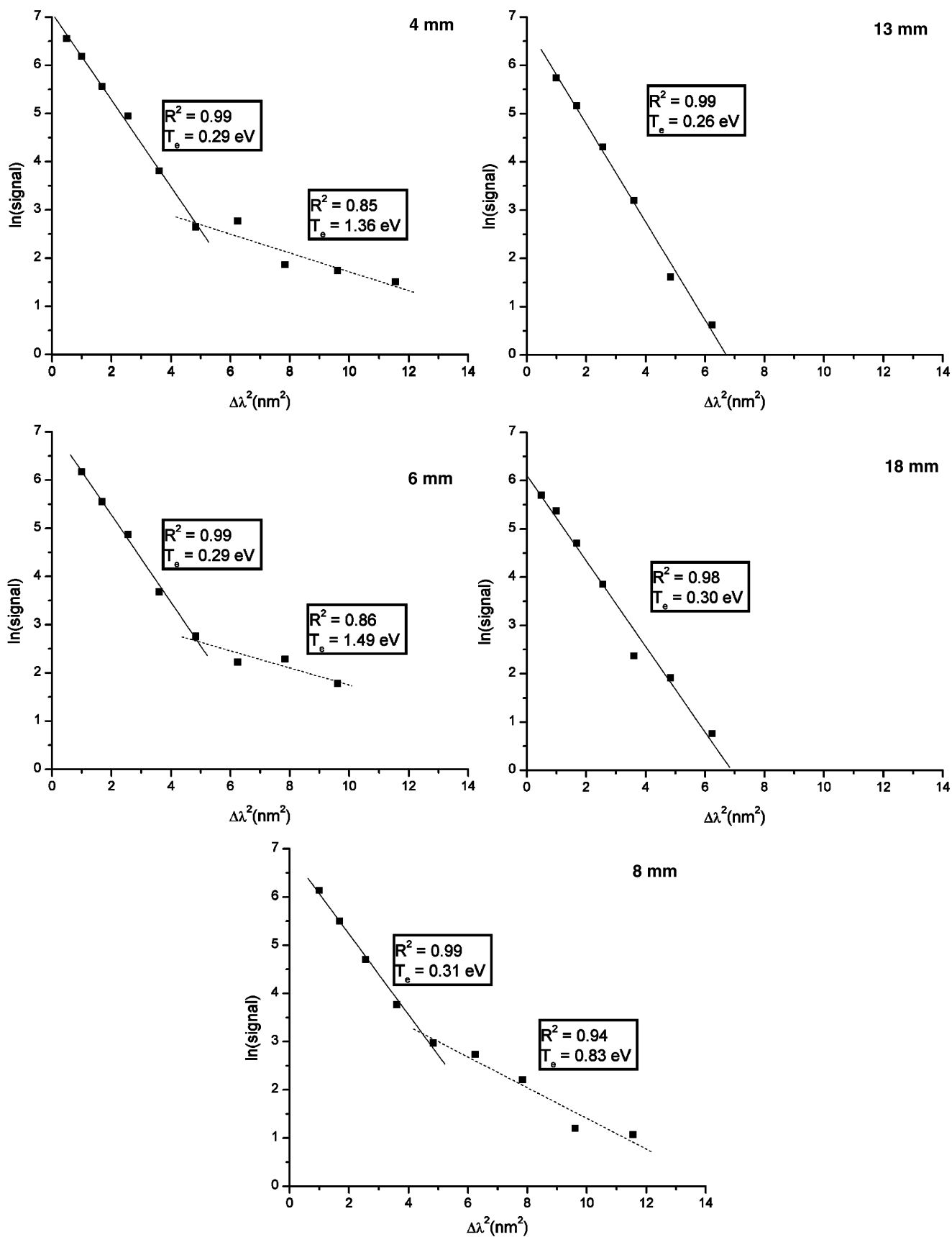


Fig. 3. Linearized Thomson-scattering spectra for d.c. glow discharge at 3 Torr, 1 kV, 55 mA taken at different distances from the cathode.

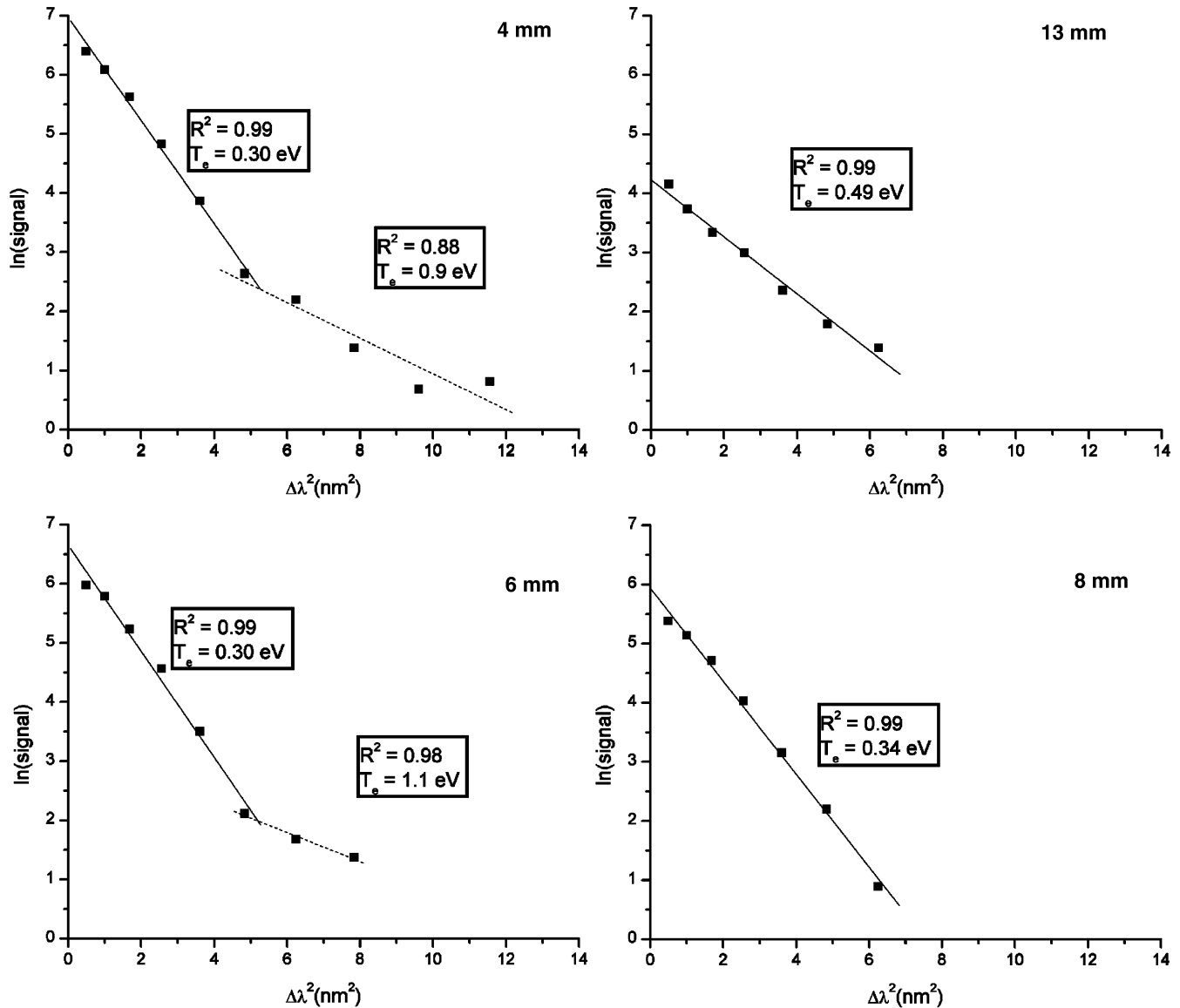


Fig. 4. Linearized Thomson-scattering spectra for d.c. glow discharge at 3 Torr, 520 V, 35 mA taken at different distances from the cathode.

zed. At this point the higher-energy electron group can no longer be observed.

Fig. 4 shows linearized Thomson-scattering spectra for several axial positions, obtained while the plasma was sustained at 3 Torr, 35 mA and 520 V. As at 55 mA and 1 kV (cf. Fig. 3), the electron energy distribution becomes increasingly Maxwellian at distances farther from the cathode. At 35 mA and 520 V (cf. Fig. 4), the negative glow is significantly smaller than at 55 mA and 1 kV, and the measured plot becomes linear closer to the cathode (at 8 mm in Fig. 4 rather than 13 mm in Fig. 3). Moreover, the Thomson-scattering spectrum was not observable at 18 mm from the cathode at 35 mA under our experimental settings. At 4, 6 and 8 mm the  $T_e$  derived from the first channels of the 35 mA spectra (Fig. 4) were approximately 0.3 eV, which again

corresponds to thermalized electrons. In contrast, the  $T_e$  associated with the tails of the spectra at 4 mm and 6 mm were 0.9 eV and 1.1 eV, respectively. Not surprisingly, the temperature of the high-energy electron group is less at lower currents and voltages. At 13 mm, in the outskirts of the negative glow, the electron temperature determined (0.5 eV) was higher than the temperatures associated with thermalized electrons in the bulk of the negative-glow region. We did not see this effect in the 55 mA case. However, the signal-to-noise ratio is much lower in the 35 mA case, so this apparent behavior should be interpreted with caution.

The linearized Thomson scattering spectra taken at 1 Torr (5 mA and 600 V) are depicted in Fig. 5. A trend of thermalization as we move away from the cathode is observed, just as with the spectra taken under other

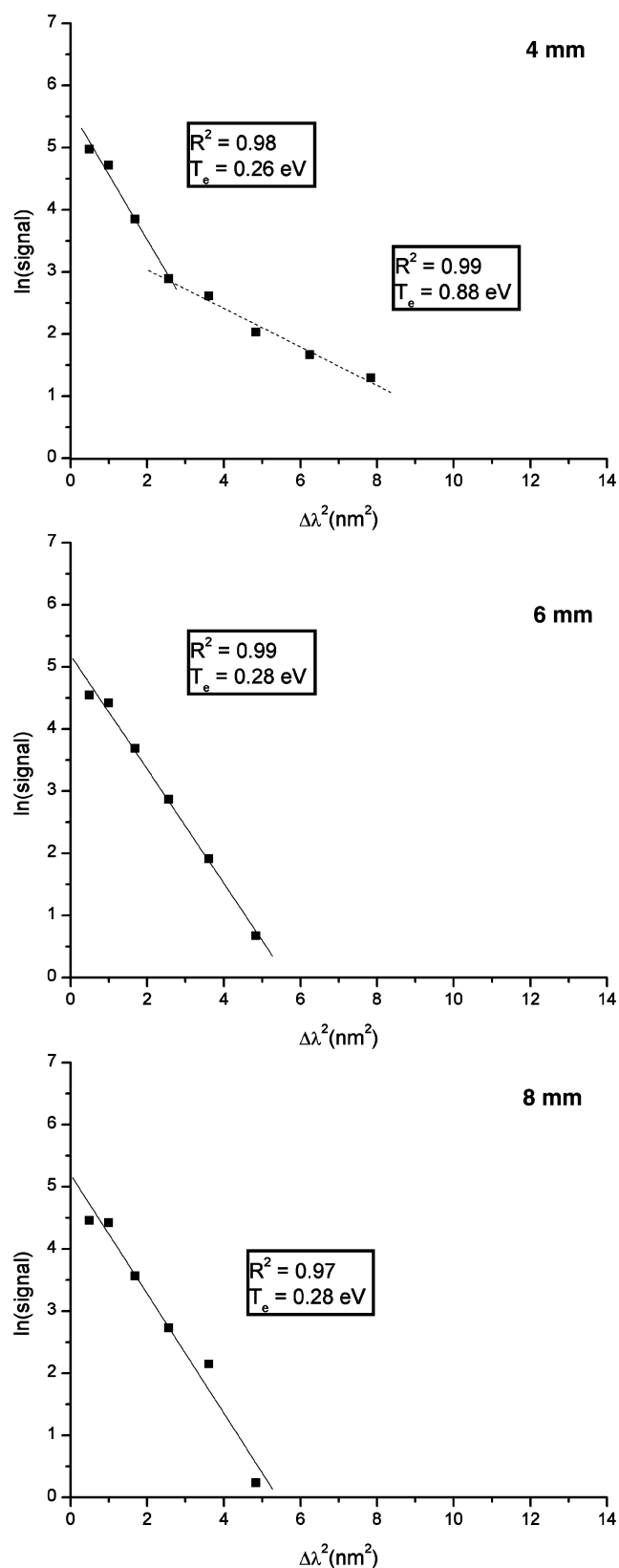


Fig. 5. Linearized Thomson-scattering spectra for d.c. glow discharge at 1 Torr, 600 V, 5 mA taken at different distances from the cathode.

conditions (cf. Figs. 4 and 5). The thermalized electrons have temperatures approximately 0.28 eV and, at 4 mm from the cathode, the tail of the spectrum shows electrons with a temperature of 0.88 eV. Even though photon counts were collected for 15 min at each wavelength channel (three times as long as for the spectra at 3 Torr), we could not obtain reasonable signals at 13 or 18 mm from the cathode.

There are similarities between the electron temperatures measured here and those obtained by other techniques. For example, Fang and Marcus [4] reported electron temperatures approximately 0.3 eV for a planar-diode d.c. glow discharge at 3 Torr of argon and 15 mA (47.4 mA/cm<sup>2</sup>) obtained via Langmuir probe. In addition, they saw a decrease in  $T_e$  as the discharge was probed at greater distances from the cathode. Moreover, when the current was increased from 10 to 22 mA (3.17 to 69.5 mA/cm<sup>2</sup>) they saw no change in  $T_e$  at 5.4 mm from the cathode at 3 Torr. This is similar to our case for short distances from the cathode, where the thermalized electron temperature did not change significantly when the current was adjusted. Angstadt et al. [28] also used a Langmuir probe and obtained  $T_e$  values ranging from ~0.26 to 0.6 eV from a pin-type glow discharge for argon pressures of ~0.5 to 1.5 Torr and operating currents of 1–3 mA (56.7 to 167 mA/cm<sup>2</sup>). Bogaerts et al. [6] studied a Grimm-type glow discharge and performed Langmuir-probe measurements that yielded  $T_e$  values ranging from ~0.2 to 0.5 eV for thermalized electrons (2 to 100 mA/cm<sup>2</sup>) and saw no significant influence from pressure changes. In addition, they reported  $T_e$  values from ~3.5 to 6.5 eV, which were attributed to secondary electrons.

We determined the EEDF shape from the Thomson-scattering spectra by the method of Huang et al. [29]. In short, the shape is obtained when the intensity difference between adjacent wavelength channels is plotted vs. the corresponding energy. In addition, in order to better compare EEDFs we normalized each one to the measured  $n_e$ . In this manner discrepancies in signal level will not obscure differences in EEDF shape. It is important to note that the resolution of the EEDF is limited by the size of the wavelength channel, in our case 0.3 nm, which was chosen with the signal level in mind. From Fig. 6 (3 Torr, 55 mA, 48.7 mA/cm<sup>2</sup>), it seems that the low-energy portion of the EEDF does not change, but the high-energy tail disappears as we examine farther from the cathode. This might be the result of low signal levels, however, rather than a true absence of high-energy electrons.

Even though we cannot observe the high-energy electrons that are responsible for ionization processes, we can clearly measure the thermalized electrons that are most important for current transport and space charge. It must also be kept in mind that all these measurements are made within the quasi-neutral nega-

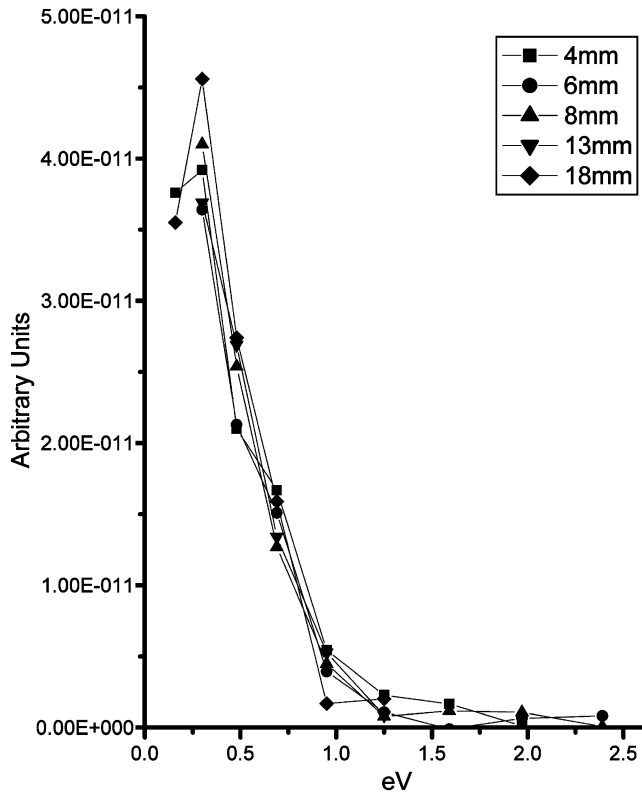


Fig. 6. Axial profile of the EEDF shape at 3 Torr, 55 mA and 1 kV.

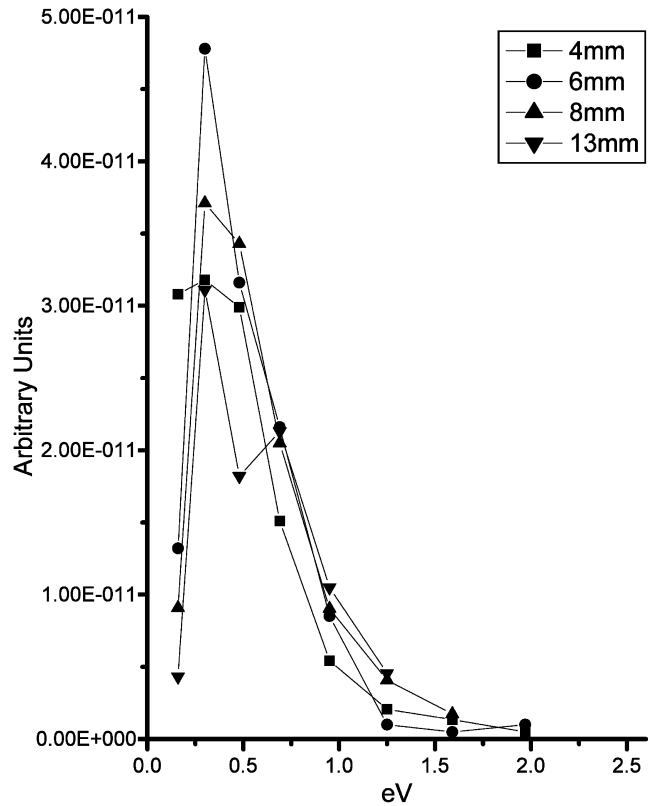


Fig. 7. Axial profile of the EEDF shape at 3 Torr, 35 mA and 520 V.

tive glow. Fang and Marcus [4] obtained EEDFs along the axis of the negative-glow region at 2 Torr (for both 37.9 and 47.4 mA/cm<sup>2</sup>), which were very similar to each other. However, at 3 Torr (47.4 mA/cm<sup>2</sup>) they found a steady lowering of the EEDF. At the same current density we observe this trend only in the high-energy tails but not among the low-energy electrons.

Fig. 7 shows that when we reduce the current from 55 to 35 mA (31 mA/cm<sup>2</sup>) and the operating voltage from 1 kV to 520 V (16.1 W/cm<sup>2</sup>) we are not able to observe the high-energy tails above 2 eV. However, we can observe a reduction in the low-energy electrons from 6 to 13 mm. Taking into account the higher density of Ar atoms, implied by the lower  $T_g$  under these conditions (compared to the 55 mA case), we can attribute the decrease to greater collisional frequencies.

Fig. 8 depicts the EEDF at different distances from the cathode for the discharge operated at 1 Torr, 5 mA, and 600 V. The only appreciable change between the different distances studied is that at 6 and 8 mm the higher-energy tails are not observable. However, a narrower low energy peak (compared to the 3 Torr cases) is apparent. This is reasonable considering the lower current (4.43 mA/cm<sup>2</sup>) and power (2.7 W/cm<sup>2</sup>) densities that exist at 1 Torr.

Fig. 9 shows the  $n_e$  axial profiles obtained at 3 Torr and 55 mA. The  $n_e$  values have been separated according

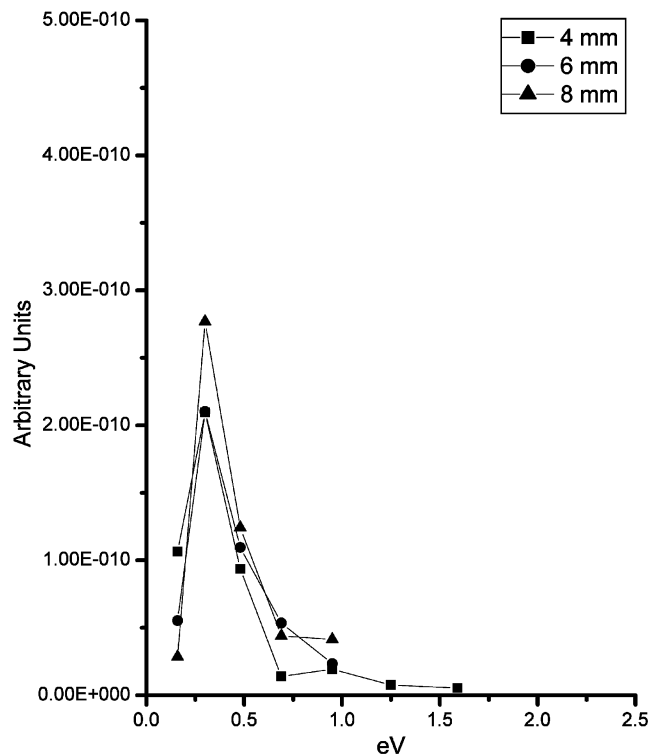


Fig. 8. Axial profile of the EEDF shape at 1 Torr, 5 mA and 600 V.

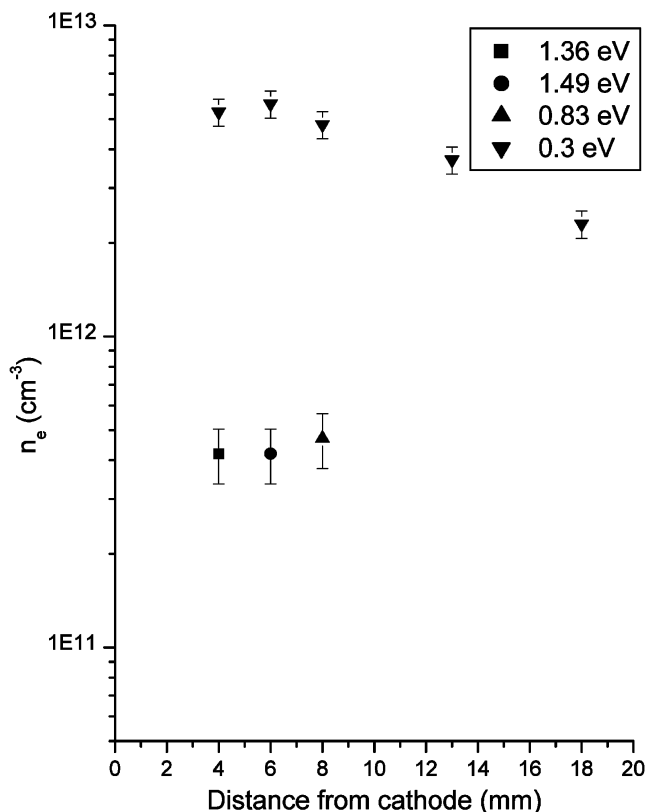


Fig. 9. Electron number density as a function of distance from the cathode at 3 Torr, 1 kV, 55 mA.

to electron energy, taken from the responding values. The thermalized electrons (those at 0.3 eV) have number densities that are at least an order of magnitude greater than those of the higher-energy electrons. In addition, the electron number density of the thermalized electrons goes down as the observation point is moved farther from the cathode. In contrast, the higher-energy electron density does not seem to change appreciably with distance from the cathode but their respective  $T_e$  does appear to drop.

From Fig. 10, which shows  $n_e$  at 35 mA, one can see that the electron number density for the thermalized electrons (those at 0.3 eV) drops more markedly as a function of distance from the cathode than it does at 55 mA (cf. Fig. 9). This rapid drop of the electron density is in agreement with calculated results (see paper II [14]). The higher-energy electron density also drops from 4 to 6 mm from the cathode. Furthermore, at 13 mm we could observe only a lower electron number density for thermalized electrons of somewhat higher energies (0.49 eV rather than 0.3 eV). It must be borne in mind, however, that the weak signals at this height and under these operating conditions generate greater error in both  $T_e$  and  $n_e$  than in the rest of the measurements.

The  $n_e$  axial profile at 1 Torr, 5 mA, and 600 V is depicted in Fig. 11. It is evident that both the thermalized and higher-energy electrons are about one order of magnitude lower in concentration at 1 Torr than at 3 Torr. However, the decline in  $n_e$  as we move away from the cathode can still be observed.

The absolute values for which different methods seem to disagree the most are those for  $n_e$ , even under comparable operating conditions. For example, at 2 mm from the cathode, Ferreira et al. [7] found electron number densities ranging from  $1.25 \times 10^{14}$  to  $3.25 \times 10^{14}$  cm $^{-3}$  in a Grimm-type glow discharge (from 93 to 148 W/cm $^2$ ) via Stark broadening of the  $H_\beta$  line. Brackett et al. [30] obtained  $n_e$  ranging from  $\sim 2 \times 10^{14}$  to  $7 \times 10^{14}$  cm $^{-3}$  for a d.c. planar-diode discharge (6.3 to 25.3 mA/cm $^2$ ) by the same technique. At 1 mm from the cathode, Kuraica et al. [8] used the same method and reported  $n_e$  for a Grimm-type glow discharge that ranged from  $1.01 \times 10^{14}$  cm $^{-3}$  at the center of the discharge to  $\sim 1 \times 10^{13}$  cm $^{-3}$  at 0.8 mm from the axial position (at 88.8 mA/cm $^2$  or 33.3 W/cm $^2$ ).

The Langmuir-probe technique gives different values than does Stark broadening of the  $H_\beta$  line. For example, Fang and Marcus [4] used a probe to determine axial profiles of  $n_e$  for a planar-diode d.c. glow discharge (3

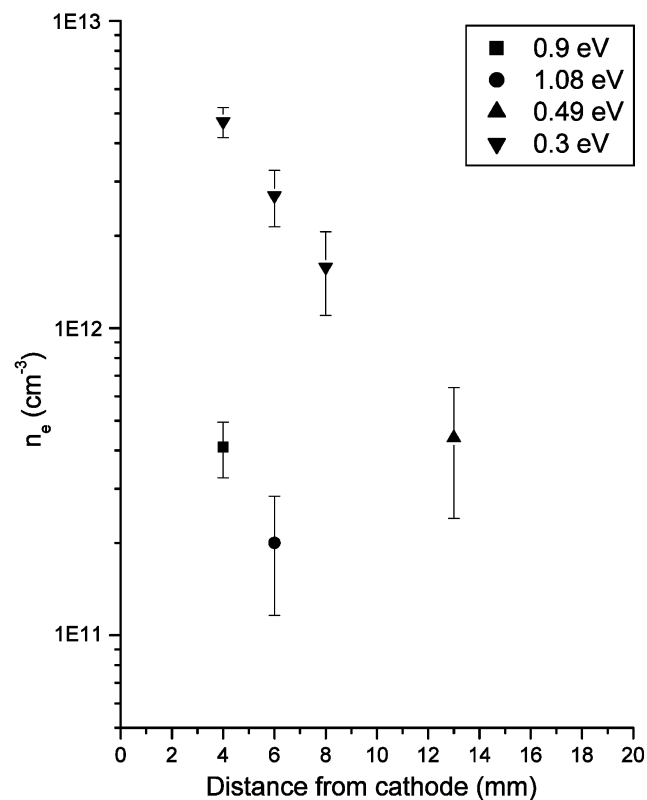


Fig. 10. Electron number density as a function of distance from the cathode at 3 Torr, 520 V, 35 mA.

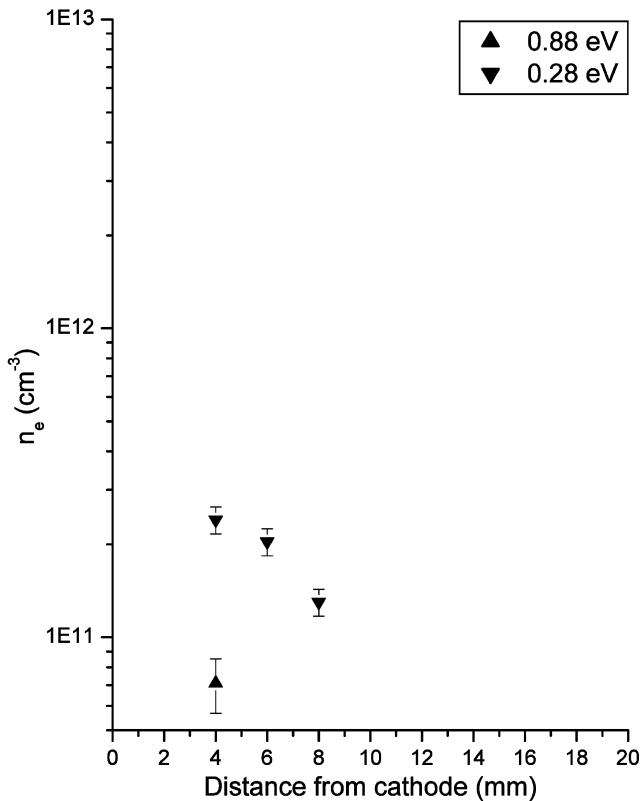


Fig. 11. Electron number density as a function of distance from the cathode at 1 Torr, 600 V, 5 mA.

Torr and 15 mA;  $47.4 \text{ mA/cm}^2$ ) and found little or no change from 5 to 14 mm away from the cathode (approx.  $2 \times 10^{11} \text{ cm}^{-3}$ ) and then a small drop to  $\sim 1.4 \times 10^{11} \text{ cm}^{-3}$  at 18 mm. Furthermore, they saw a small increase in  $n_e$  at 2 Torr as the current was raised from 12 to 15 mA, which is similar to what we observe. Angstadt et al. [28] also used Langmuir probes and found  $n_e$  a couple of orders of magnitude lower ( $1 \times 10^9$  to  $3 \times 10^9 \text{ cm}^{-3}$ ) for a pin-type glow discharge at  $\sim 1$  Torr and 2 mA ( $111 \text{ mA/cm}^2$ ). Bogaerts et al. [6] used the same method in a Grimm-type glow discharge and reported  $n_e$  values 7 mm from the cathode ranging from  $\sim 1 \times 10^{12}$  to  $4 \times 10^{14} \text{ cm}^{-3}$ , depending on the pressure and voltage applied (2 to  $100 \text{ mA/cm}^2$ ). Furthermore, Monte Carlo fluid-modeling calculations of a Fisons VG 9000 glow discharge cell yielded  $n_e$  between  $10^{11}$  and  $10^{12} \text{ cm}^{-3}$  (at approx. 0.75 Torr;  $4.5 \text{ mA/cm}^2$ ) for slow electrons [31]. In addition, our measured electron densities are compared with calculated results, and the agreement is quite reasonable (see paper II [14]).

To be fair, most of the geometries in the above-referenced studies are different from the one in the present study. The Fang and Marcus studies [4,5] bear the strongest similarities to our setup. In the case of  $n_e$ , their values are about an order of magnitude lower than those we obtain for thermalized electrons at 3 Torr and

comparable current densities. However, it has been shown [9] that Langmuir probes can reduce the  $n_e$  values by as much as 50% due to the presence of the probe. In addition, the coating of the probe might introduce some error. Taking this possibility into account, and the small but real differences in operating conditions, the disparity in values between the two sets of investigations is not surprising.

It is evident that the gas-kinetic temperature and the electron properties are related when the axial profiles for both are examined. At 3 Torr and 30 mA,  $T_g$  goes down dramatically over the first 13 mm from the cathode (cf. Fig. 2). At 35 mA, the  $n_e$  also decreases markedly from 4 to 13 mm (cf. Fig. 10). However, at 50 mA,  $T_g$  changes very little from 6 to 18 mm (cf. Fig. 2) and the change in  $n_e$  at 55 mA (cf. Fig. 9) over these same distances is also very small compared to the change at 35 mA (cf. Fig. 10).

This difference might be due to changes in gas density associated with the respective temperatures that affect the mean free path and the frequency of collisions. At greater distances from the cathode, electrons will have already experienced several energy-depleting collisions, so there will be fewer electron-impact ionization events. Thus, there will be lower ion densities and, since argon ions are the species mainly responsible for imparting energy to neutral argon by elastic collision, there will be lower gas-kinetic temperatures in this region. At higher operating currents and voltages there will be more efficient secondary emission of electrons from the cathode. These electrons will have high energies and will produce more electrons from gas-phase ionization. In this way the electron number density will go up and the ion density will follow. As discussed before, the ion density will influence the density of fast argon atoms that in turn influence the gas-kinetic temperature.

#### 4. Conclusion

Laser-scattering techniques have proven to be very valuable to determine the behavior of several plasma parameters in a glow discharge. The measured gas-kinetic temperatures from Rayleigh scattering agree reasonably well with those from previous studies. Not surprisingly, when the operating current is raised,  $T_g$  goes up. In addition, at a constant current, the drop in  $T_g$  when the pressure is increased suggests lower plasma resistance since the sustaining voltage is lessened.

The non-Maxwellian behavior of the plasma is evident from linearized Thomson-scattering spectra. A thermalized group of electrons exhibit a  $T_e$  approximately 0.3 eV (approx. 3500 K) with no observable change within the negative glow as a function of current, voltage, or distance from the cathode. In contrast, a higher-energy

electron group displayed greater  $T_e$  at distances closer to the cathode, which shows that electrons lose energy as they travel through the negative glow towards the anode. In addition, the  $T_e$  for these higher-energy electrons increases when the current and voltage are raised. This suggests a more efficient emission of secondary electrons from the cathode. Finally, the interdependence of the plasma properties and species is apparent when the respective axial profiles are compared. A comparison with results from numerical modeling will be carried out in paper II [14]. Future work includes studies of how these plasma species are affected by the cathode material, addition of impurity trace gasses, as well as pulsed and boosted discharges.

### Acknowledgments

Supported in part by the US Department of Energy through Grant DE-FG02-98ER14890 and by a fellowship from Merck Research Laboratories. A. Bogaerts acknowledges financial support from the Flemish Fund for Scientific Research (FWO), and for supporting her research visit at Indiana University, as well as from the Belgian Federal Services for Scientific, Technical and Cultural Affairs (DWTC/SSTC) of the prime Minister's Office through the IUAP-V program.

### References

- [1] R.K. Marcus (Ed.), *Glow Discharge Spectroscopies*, Plenum Press, New York, NY, 1993.
- [2] R.K. Marcus, J.A.C. Broekaert (Eds.), *Glow Discharge Plasmas in Analytical Spectroscopy*, J. Wiley, Chichester, England, 2003.
- [3] A. Bogaerts, R. Gijbels, *Fundamental aspects and applications of glow discharge spectrometric techniques*, *Spectrochim. Acta Part B* 53 (1998) 1–42.
- [4] D. Fang, R.K. Marcus, *Use of a cylindrical Langmuir probe for the characterization of charged particle populations in a planar diode glow discharge device*, *Spectrochim. Acta Part B* 45 (1990) 1053–1074.
- [5] D. Fang, R.K. Marcus, *Effect of discharge conditions and cathode identity on charged particle populations in the negative glow region of a simple diode glow discharge*, *Spectrochim. Acta Part B* 46 (1991) 983–1000.
- [6] A. Bogaerts, A. Quentmeier, N. Jakubowski, R. Gijbels, *Plasma diagnostics of an analytical Grimm-type glow discharge in argon and in neon: Langmuir probe and optical emission spectrometry measurements*, *Spectrochim. Acta Part B* 50 (1995) 1337–1349.
- [7] N.P. Ferreira, H.G.C. Human, L.R.P. Butler, *Kinetic temperatures and electron densities in the plasma of a side view Grimm-type glow discharge*, *Spectrochim. Acta Part B* 35 (1980) 287–295.
- [8] M. Kuraica, N. Kinjevic, M. Platasa, D. Pantelic, *Plasma diagnostics of the Grimm-type glow discharge*, *Spectrochim. Acta Part B* 47 (1992) 1173–1186.
- [9] M.D. Bowden, M. Kogano, Y. Suetome, T. Hori, K. Uchino, K. Muraoka, *Comparison of electron property measurements in an inductively coupled plasma made by Langmuir probe and laser Thomson scattering techniques*, *J. Vac. Sci. Technol. A* 17 (1999) 493–499.
- [10] S.K. Ohorodnik, W.W. Harrison, *Plasma diagnostic measurements in the cryogenically cooled glow discharge*, *J. Anal. Atom. Spectrom.* 9 (1994) 991–996.
- [11] N.I. Uzelac, F. Leis, *Measurement of gas temperatures and metastable state densities in a microwave boosted glow discharge using a diode laser*, *Spectrochim. Acta Part B* 47 (1992) 877–887.
- [12] S.M. Rossnagel, *Gas density reduction effects in magnetrons*, *J. Vac. Sci. Technol. A* 6 (1988) 19–24.
- [13] G. Gamez, M. Huang, S.A. Lehn, G.M. Hieftje, *Laser-scattering instrument for fundamental studies on a glow discharge*, *J. Anal. Atom. Spectrom.* 18 (2003) 680–684.
- [14] A. Bogaerts, R. Gijbels, G. Gamez, G.M. Hieftje, *Fundamental studies on a planar-cathode direct current glow discharge. Part II: numerical modeling and comparison with laser scattering experiments*, *Spectrochim. Acta Part B* 59 (2004) 449–460.
- [15] R.C. Weast, M.J. Astle (Eds.), *CRC Handbook of Chemistry and Physics*, 63rd, CRC Press, Boca Raton, Florida, 1982.
- [16] T. Hori, M.D. Bowden, K. Uchino, K. Muraoka, M. Maeda, *Measurements of electron temperature, electron density, and neutral density in a radio-frequency inductively coupled plasma*, *J. Vac. Sci. Technol. A* 14 (1996) 144–151.
- [17] I. Revel, L.C. Pitchford, J.P. Boeuf, *Calculated gas temperature profiles in argon glow discharges*, *J. Appl. Phys.* 88 (2000) 2234–2239.
- [18] A. Bogaerts, R. Gijbels, V.V. Serikov, *Calculation of gas heating in direct current argon glow discharges*, *J. Appl. Phys.* 87 (2000) 8334–8344.
- [19] W. Cronrath, H. Tanaka, M.D. Bowden, K. Uchino, K. Muraoka, *Measurement of the neutral particle density in an electron cyclotron resonance plasma by Rayleigh scattering*, *Jpn. J. Appl. Phys.* 34 (1995) L1402–L1404.
- [20] A. Bogaerts, R.D. Guenard, B.W. Smith, J.D. Winefordner, W.W. Harrison, R. Gijbels, *Three-dimensional density profiles of argon metastable atoms in a direct current glow discharge: experimental study and comparison with calculations*, *Spectrochim. Acta Part B* 52 (1997) 219–229.
- [21] K.R. Hess, W.W. Harrison, *The role of metastable atoms in glow discharge ionization processes*, *Anal. Chem.* 60 (1988) 691–696.
- [22] N.P. Ferreira, J.A. Strauss, H.G.C. Human, *Distribution of metastable argon atoms in the modified Grimm-type electrical discharge*, *Spectrochim. Acta Part B* 37 (1982) 273–279.
- [23] J.A. Strauss, N.P. Ferreira, H.G.C. Human, *An investigation into the role of metastable argon atoms in the afterglow of a low pressure discharge*, *Spectrochim. Acta Part B* 37 (1982) 947–954.
- [24] C.D. West, H.G.C. Human, *Self-absorption and Doppler temperatures of emission lines excited in a glow discharge lamp*, *Spectrochim. Acta Part B* 31 (1976) 81–92.
- [25] M. Kasik, C. Michellon, L.C. Pitchford, *Effects of cathode heating in a GDMS system*, *J. Anal. Atom. Spectrom.* 17 (2002) 1398–1399.
- [26] K. Warner, G.M. Hieftje, *Thomson scattering from analytical plasmas*, *Spectrochim. Acta Part B* 57 (2002) 201–241.
- [27] W. Stern, *Grid-probe measurements in a negative glow*, *Beitr. Plasmaphys.* 9 (1969) 59–73.
- [28] A.D. Angstadt, J. Whelan, K.R. Hess, *Optical and Langmuir probe investigations of excitation temperatures in a low-*

- pressure glow discharge with variations in discharge gas identity, *Microchem. J.* 47 (1993) 206–223.
- [29] M. Huang, K. Warner, S.A. Lehn, G.M. Hieftje, A simple approach to deriving an electron energy distribution from an incoherent Thomson scattering spectrum, *Spectrochim. Acta Part B* 55 (2000) 1397–1410.
- [30] J.M. Brackett, J.C. Mitchell, T.J. Vickers, Temperature and electron density measurements in a dc glow discharge, *Appl. Spectrosc.* 38 (1984) 136–140.
- [31] A. Bogaerts, R. Gijbels, W.J. Goedheer, Hybrid Monte Carlo-fluid model of a direct current glow discharge, *J. Appl. Phys.* 78 (1995) 2233–2241.